Colloids and Surfaces B: Biointerfaces 88 (2011) 539–551

Contents lists available at ScienceDirect

Colloids and Surfaces B: Biointerfaces

journal homepage: www.elsevier.com/locate/colsurfb

Review

Immobilization of histidine-tagged proteins on electrodes

Claudia Ley[a], Dirk Holtmann[a], Klaus-Michael Mangold[b], Jens Schrader[a,*]

[a] Biochemical Engineering Group, Karl-Winnacker-Institut, DECHEMA e.V., Theodor-Heuss-Allee 25, 60486 Frankfurt am Main, Germany
[b] Electrochemistry Group, Karl-Winnacker-Institut, DECHEMA e.V., Theodor-Heuss-Allee 25, 60486 Frankfurt am Main, Germany

ARTICLE INFO

Article history:
Received 3 May 2011
Received in revised form 19 July 2011
Accepted 19 July 2011
Available online 26 July 2011

Keywords:
Protein immobilization
His-tagged protein
Biosensor
Electrode modification
SAM
Conductive polymers
Electroenzymatic processes

ABSTRACT

The development of new enzyme immobilization techniques that do not affect catalytic activity or conformation of a protein is an important research task in biotechnology including biosensor applications and heterogeneous reaction systems. One of the most promising approaches for controlled protein immobilization is based on the immobilized metal ion affinity chromatography (IMAC) principle originally developed for protein purification. Here we describe the current status and future perspectives of immobilization of His-tagged proteins on electrode surfaces. Recombinant proteins comprising histidine-tags or histidine rich native proteins have a strong affinity to transition metal ions. For metal ion immobilization at the electrode surface different matrices can be used such as self-assembled monolayers or conductive polymers. This specific technique allows a reversible immobilization of histidine-tagged proteins at electrodes in a defined orientation which is an important prerequisite for efficient electron transfer between the electrode and the biomolecule. Any application requiring immobilized biocatalysts on electrodes can make use of this immobilization approach, making future biosensors and biocatalytic technologies more sensitive, simpler, reusable and less expensive while only requiring mild enzyme modifications.

Contents

1. Introduction 539
2. Analytics 540
3. Conductive polymers 540
   3.1. Use of functionalized monomers with coordination sites for metal ions 540
   3.2. Postfunctionalization of conductive polymers creating sites for metal ion binding 541
4. Self-assembled monolayers of organosulfur compounds on gold electrodes 542
   4.1. NTA-terminated SAMs 542
   4.2. The DTSP–ANTA system 545
      4.2.1. Immobilization of photosynthetic reaction center 545
      4.2.2. Immobilization of rhodopsins 547
      4.2.3. Immobilization of cytochrome c oxidase 547
   4.3. Alternatives to NTA 548
5. Further electrode surface modification methods 548
6. Outlook 550
7. Conclusion 550
Acknowledgement 550
References 550

1. Introduction

Among all protein tags the (hexa)histidine-tag is one of the most prominent affinity tags established especially in protein purification [1] since it has a small size and does usually not interfere with structure and function of the protein [1]. Furthermore the immobilization via a histidine-tag is reversible and the surface can be regenerated under mild conditions employing imidazole as competitive ligand (or any other ligand being a Lewis base), acidic pH or even a chelating ligand like EDTA allowing for metal ion exchange [2]. The immobilization via a histidine-tag is highly specific. Theoretically only the protein of interest will be immo-

* Corresponding author.
E-mail address: schrader@dechema.de (J. Schrader).

0927-7765/$ – see front matter © 2011 Elsevier B.V. All rights reserved.
doi:10.1016/j.colsurfb.2011.07.044

bilized while non-specific binding of other, non-tagged proteins, will be avoided [3]. Because of the high affinity it is generally possible to work with low biomolecule concentrations [4]. The position of the histidine-tag at the protein surface can be controlled by genetic engineering resulting in oriented immobilization of the protein [5]. This approach is applicable to different protein types [5] and creates uniformly oriented protein layers. In this way an increased efficiency of the interaction of the immobilized protein with the solution phase or the solid support can be expected since, e.g. the active sites are facing in one direction and are all contributing to the biosensor response [2]. This uniform orientation is of special interest for several applications, e.g. for the immobilization of membrane proteins which often have an asymmetric functionality [6]. Protein orientation plays also a key role in the immobilization of redox proteins because the efficiency of direct electron transfer is strongly influenced by the orientation of the protein at the electrode surface [4,7]. In comparison immobilization strategies involving chemical modification of biomolecules, which are for example an integral part of covalent attachment methods, can result in high biomolecule densities at the surface and multipoint attachments neutralizing enzyme active sites [3,8]. Additionally chemical grafting can alter the three-dimensional enzyme morphology and especially in case of entrapment methods often mass-transfer limitations occur [8]. In contrast immobilization strategies based on affinity methods have the advantage of preserving enzyme activity upon immobilization with the spatial distribution being well controlled by the concentration of the binding molecules at the electrode surface [4,9]. Compared to other affinity approaches His-tag immobilizations seem to be more stable than, e.g. those based on GST-tags, which additionally are larger and have a stronger influence on protein functionality.

2. Analytics

The immobilization of histidine-tagged proteins on electrodes is a multistep process requiring different analytical tools to determine electrode surface properties, chemical composition and surface coverage. Besides standard techniques comprising surface plasmon resonance (SPR) and ellipsometry [10] also methods are used to elucidate the elemental composition of the surface including energy dispersive X-ray spectroscopy (EDX) or X-ray photoelectron spectroscopy (XPS) [4,5]. In addition surface-enhanced infrared absorption spectroscopy (SEIRAS) [7] and surface-enhanced resonance Raman spectroscopy (SERR) [11] as well as imaging methods such as scanning electron microscopy (SEM) [12], atomic force microscopy (AFM) [8] and scanning force microscopy [5] are powerful tools for surface analysis. In combination with electrochemistry the electrochemical quartz crystal microbalance (EQCM) and impedance spectroscopy are noteworthy, the former yielding information about mass changes at the surface in nanogram scale.

3. Conductive polymers

Conductive polymers are a common material used for surface modification of electrodes since the monomers, which are commercially available in great variety, can be electropolymerized at the electrode surface. The resulting polymer film is inherently conductive and its film thickness can be controlled by the electrochemical reaction conditions applied [13,14]. A well studied example is polypyrrole (PPy), which is biocompatible and can be polymerized in aqueous medium at neutral pH [15].

3.1. Use of functionalized monomers with coordination sites for metal ions

A pyrrole monomer functionalized with nitrilotriacetic acid (NTA) has been used to coordinate copper cations and subsequently histidine-tagged glucose oxidase [16]. The monomer was prepared by a two step carbodiimide coupling reaction between 1-(11-undecanoic acid) pyrrole and nitrilotriacetic acid (Table 1). Copper coordination was achieved at slightly acidic pH and copper concentration was determined after overoxidation of the polymer leading to loss of its electroactivity and hence reducing the background current. Copper concentration was observed to be related to the thickness of the polymer film in a close to linear manner resulting in an average value of 3.5 NTA groups per coordinated copper cation. After incubation of the copper loaded polymer films with histidine-tagged glucose oxidase a maximum current density of 3.4 $\mu A\,cm^{-2}$ was obtained for hydrogen peroxide oxidation at the electrode which is generated by the enzyme when oxidizing glucose. The same experiment with non-tagged glucose oxidase yielded a maximum current density of 0.48 $\mu A\,cm^{-2}$ proving the specific immobilization via the histidine-tag being effective. By treatment with imidazole approximately 88% of the histidine-tagged enzyme could be eluted from the copper loaded film. Reversibility of this approach was shown for five successive cycles of enzyme loading and elution. The authors emphasize that no potentials below −0.5 V vs. SCE can be applied to this assembly because of copper reduction and also an acidic pH below 4 can impede copper coordination. This work has been extended to the fabrication of PPy-NTA nanotubes [17]. A single nanotube was employed to connect two gold electrodes building a sensor for the detection of copper and consequently pentahistidine tagged synthaxin protein. The normalized change in resistance at −500 mV was determined to be a linear function of $\log[Cu^{2+}]$ and the signal was not disturbed by alkali metal ions such as Na^+. But the sensor is not selective against other transition metal ions such as nickel or cadmium which can also be chelated by NTA. When adding the tagged synthaxin protein to the sensor assembly the resistance of the copper loaded PPy–NTA nanotube increases until saturation is achieved around 100 $ng\,mL^{-1}$. Selectivity was proven by testing the sensor with bovine serum albumin (BSA) in concentrations up to 10 $mg\,mL^{-1}$ without obtaining a sensor response. The same approach was used to develop a DNA sensor [18]. Histidine-tagged oligonucleotides binding to the copper loaded PPy-NTA polymer film were employed to immobilize a certain DNA target. The hybridization process was confirmed by fluorescence microscopy, QCM and amperometric measurements. After hybridization with a biotin labeled cDNA a fluorescence marked avidin was added which allowed detection of the hybridization process by fluorescence microscopy. A surface density of $1.7 \times 10^{-11}\,mol\,cm^{-2}$ for the histidine-tagged oligonucleotide was determined by QCM studies with successive hybridization taking place in a ratio of 45%. Binding of avidin to the hybridized DNA yielded a coverage of $7.4 \times 10^{-12}\,mol\,cm^{-2}$ which corresponds to a monolayer coverage of avidin. Furthermore incubation of this assembly with biotinylated glucose oxidase – which produces hydrogen peroxide when oxidizing glucose – led to the amperometric detection of hydrogen peroxide oxidation at the electrode with a glucose sensitivity of 0.5 $mA\,cm^{-2}\,mol^{-1}\,L$ and a maximum current density of 9.5 $\mu A\,cm^{-2}$. The authors concluded that the polymer film's hydrophilic character facilitates hydrogen peroxide diffusion and that the maximum current density achieved indicates a compact enzyme layer formation. The maximum current density measured at glucose saturation conditions remains stable for 1 h proving the stability of the whole system including the NTA–copper–histidine system. Interestingly Baur et al. [19] showed that the same PPy–NTA system chelating copper can be used to immobilize biotinylated biomolecules

Table 1
Structures of conductive polymers, that are capable of complexing metal cations, used for the immobilization of histidine-tagged biomolecules.

Polymer structure	Interface	His-tagged biomolecule	Reference
(a) Conductive polymers out of functionalized monomers			
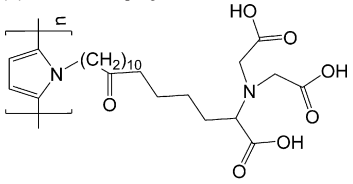 *Γ = 41000 pmol cm^{-2} [16]** *Γ = 1500 pmol cm^{-2} [18]**	Cu^{2+} Cu^{2+} Cu^{2+}	Glucose oxidase Synthaxin Oligonucleotides (Γ = 17 pmol cm^{-2})[a]	[16] [17] [18]
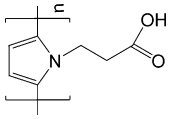	Ni^{2+}	Alkaline phosphatase	[20]
(b) Postfunctionalized conductive polymers			
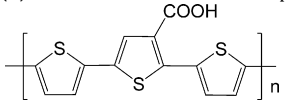	Anti-His_6 antibody	Mismatch repair proteins MutH and MutL	[23]
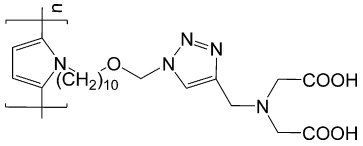	Cu^{2+}	Insulin	[24]

Γ = maximal surface coverage.
[a] Values have been converted to make units comparable.

without avidin as intermediating affinity counterpart. This idea is based on the fact that the thioether group of biotin can coordinate to metal ions in solution. This approach was further confirmed by immobilizing a biotinylated polyphenol oxidase whose analytical performance was tested with catechol and yielded a catechol sensitivity of 656 mA mol^{-1} L cm^{-2} and a maximum current density of 25.4 μA cm^{-2}.

Besides the common chelating group NTA also carboxylic acid groups can coordinate to transition metal ions. One of the well studied carboxylic acid derivatives of pyrrole is 3-(pyrrole-1-yl) propanoic acid (PPA) (Table 1), in which the hydrogen atom of the pyrrole nitrogen has been substituted by propanoic acid [20,21]. Reflectance angle infrared spectra showed that nickel is coordinated by the carboxyl groups in an unidentate and concentration dependent manner [20]. Assuming an octahedral coordination state of nickel two binding sites will be occupied by carboxyl groups of the polymer leaving four binding sites open which will be occupied by water molecules and can be easily displaced by stronger ligands like histidine residues on a protein. Furthermore it was proven that the polymer film is porous and allows ion diffusion to the backside of the film [20,22]. The interaction between nickel cations and carboxyl groups is rather weak but resists sequestering in 25 mM phosphate buffer at pH 7 [20] and water over several hours [21]. Under acidic conditions nickel cations are eluted due to protonation of the carboxylic acid groups. Subsequently polyhistidine and a histidine-tagged alkaline phosphatase have been immobilized at the nickel loaded polymer [20]. Changes in the XPS spectra related to the Ni($2p_{3/2}$) line indicate interaction of the bound nickel with the histidine residues of the molecules. Additionally the histidine-tagged alkaline phosphatase remained active in the polymer bound state which was confirmed by an activity assay yielding K_m = 2.5 mM and V_{max} = 187 μmol s^{-1} cm^{-2} [20]. This approach may be a promising candidate for establishing a direct electrochemical communication between the immobilized enzyme and the electrode but has not been tested yet in this regard.

3.2. Postfunctionalization of conductive polymers creating sites for metal ion binding

A common approach for cross-linking biomolecules is carbodiimide chemistry which has the advantage of activating a reaction between carboxyl and amine groups forming an amide bond without introduction of an additional spacer. Since monomers having carboxylic acid groups are readily available carbodiimide treatment is a suitable and popular method to chemically graft a polymer film. Darain et al. [23] used carbodiimide chemistry to modify a polymer which exposes carboxylic acid groups, namely poly(5,2′:5′2″-terthiophene-3′-carboxylic acid) (polyTTCA) (Table 1). An epitope specific monoclonal anti-His_6 antibody has been covalently linked to the conductive polymer layer. After fabrication the polyTTCA-antibody electrode was blocked with BSA and exposed to a solution containing one of the histidine-tagged mismatch repair proteins MutH and MutL. The interaction between the histidine-tagged proteins and the antibody-modified polymer has been studied by impedance spectroscopy and QCM studies. The impedance spectra clearly showed a decrease in impedance for the modified electrodes incubated with His-MutH and His-MutL while for untagged MutH and MutL no changes were observed. In QCM experiments a mass change of 987 ± 1 ng cm^{-2} was determined upon binding of His-MutL to a polyTTCA-antibody modified quartz with equilibration reached after approximately 1 h. For non-tagged MutL only 3.6% of the aforementioned value was reached related to non-specific protein binding. Under optimal conditions for the immunoreactions linear calibration plots for both His-tagged MutH and His-tagged MutL were obtained with linear ranges from 50 to 150 and, respec-

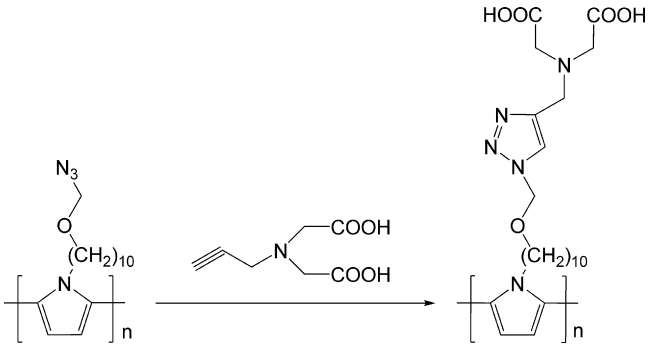

Fig. 1. Click-reaction producing an iminodiacetic acid modified polypyrrole [24].

tively, 250 μg mL^{-1} and detection limits of 37.8 for his-tagged MutH and 59.12 μg mL^{-1} for his-tagged MutL [23].

One promising approach for introducing functional groups on a conductive polymer is click chemistry. Therefore the monomer has to offer azide or alkyne groups which are thermally stable and inert in electrochemical experiments [24]. These groups remain unaltered upon electropolymerization of the monomer yielding the conductive polymer backbone and are the reactive sites for the following click chemistry modification. That way Li et al. synthesized the pyrrole monomer N-(10-azidodecyl)pyrrole (Table 1) and polymerized the monomer electrochemically in acetonitrile. Afterwards the polymer was converted with N-propargyl iminodiacetic acid in a copper catalyzed Huisgen 1,3-dipolar cycloaddition introducing iminodiacetic acid (IDA) as chelating group (Fig. 1).

Since copper is used as catalyst for the click reaction the polymer ligates the metal via the IDA groups already after synthesis. Furthermore fluorescence marked and hexahistidine-tagged insulin was added and strong fluorescence was observed using a fluorescence microscope. Upon treatment with imidazole the fluorescence diminishes significantly proving the specific immobilization of insulin.

4. Self-assembled monolayers of organosulfur compounds on gold electrodes

Organosulfur compounds coordinate strongly to transition metal surfaces and adsorb as a monomolecular layer [25] in a process called self-assembly. Monolayers of alkanethiolates on gold are probably the most studied ones and offer a high versatility in the available tailgroup chemistry. Monolayer deposition is generally achieved by soaking the electrode in a solvent like ethanol or DMSO containing the monolayer molecules which subsequently self-assemble at the gold surface in a time course of several hours [25]. Hence the preparation of self-assembled monolayers (SAMs) is experimentally facile and allows a flexible structuring of surfaces [25].

4.1. NTA-terminated SAMs

One of the most common tailgroups used to immobilize metal cations and subsequently histidine-tagged proteins is NTA or derivatives thereof. For example the short-chain thiol N-[5-(1,2-dithiolan-3-ylpentanoylamino)-1-carboxypentyl]iminodiacetic acid was synthesized by Balland et al. [26] to immobilize histidine-tagged laccase (Table 2). Via oxidative desorption of the monolayer a sulfur atom surface coverage of 700 ± 50 pmol cm^{-2} was determined which is comparable to theoretical values given for a close packed monolayer. Accordingly the surface concentration of the chelating NTA groups was estimated to be 350 ± 25 pmol cm^{-2}. Around 70% of these groups were found to be chelating copper yielding a metal ion coverage of 250 ± 50 pmol cm^{-2}. In combination with the histidine-tagged enzyme a catalytic wave was obtained in cyclic voltammetry experiments when the solution contains the one electron mediator [Os(bpy)2pyCl]$^{2+}$. In experiments without using the mediator neither N- nor C-terminal tagged laccase seemed to communicate directly with the electrode. Determination of enzyme binding kinetics showed a maximum current response after an incubation time of 90 min with the signal being stable for 2 h and finally followed by a signal decrease. This is a general phenomenon observed at enzyme-NTA modified electrodes related to competitive binding of the metal cation by the histidine-tag of the enzyme [26]. When loading the monolayer with nickel instead of copper maximal current densities 3.5-fold lower than with copper were obtained but showing similar kinetic properties indicating a poorer interaction of the histidine-tag with the nickel–NTA complex. The same SAM NTA system was used to immobilize the small, histidine-tagged hemoprotein human neuroglobin (hNb), which has an accessible heme site and is similar in size to cytochrome *c* [27]. After preparation of the monolayer and immersion in nickel solution the free coordination sites were determined with the redox probe 1,1′-bis(N-imidazolylmethyl)ferrocene. The redox probe showed good binding abilities and electron transfer properties and furthermore an electron transfer rate of 80 s^{-1} and a SAM thickness of around 19 Å were determined. But for binding of hNb no oxidation or reduction peak in cyclic voltammetry was obtained, in both air free and air saturated solutions. Surface enhanced resonance Raman (SERR) spectra revealed that the immobilized protein is not altered in its native structure and in contrast to the cyclic voltammetry experiments direct electric contact between the electrode and the protein has been seen with a rate constant of 0.12 s^{-1}. Madoz-Gúrpide et al. [5] immobilized the enzyme ferredoxin:NADP$^+$ reductase (FNR) on an nitrilotriacetic acid terminated SAM. The monolayer was prepared by self-assembly of dithioctic acid (TOA). Its carboxylic acid terminal groups were activated by esterification with N-hydroxysuccinimide to facilitate the reaction with N-(5-amino-1-carboxypentyl)iminodiacetic acid (ANTA) yielding an NTA terminated surface (Table 2). By reductive desorption the surface coverage of the NTA modified monolayer was determined yielding 7.2 ± 0.6 × 10^{-10} mol cm^{-2}. Copper chelation by the TOA-ANTA monolayer was proven by XPS measurements and after reductive desorption in alkaline media atomic emission spectroscopy (AES-ICP) was performed yielding a copper concentration of 2.8 × 10^{-10} mol cm^{-2} which correlates to 80% of the dithioctic chains being complexed to copper ions. The binding of two mutant FNR proteins exhibiting a histidine pair at a surface exposed α-helix was investigated by analysis of their diaphorase activity with NADPH as electron donor and ferricinium methanol as electron acceptor. The oxidized ferricinium methanol is generated at the electrode during the anodic scan in cyclic voltammetry. Only electrodes treated with the genetically modified FNR proteins gave an electrochemical response in the presence of NADPH and ferricinium methanol while the wild type did not. In the second step of the monolayer preparation an ANTA/ethanolamine mixture was used to be coupled to the dithioctic acid since the authors assume a steric hindrance of protein binding in an undiluted monolayer system. The amount of immobilized protein was determined from activity measurements and an ELISA assay after elution with imidazole. Specificity of protein binding was proven by elution of the protein by imidazole as well as EDTA treatment. Furthermore the monolayer without copper did not immobilize the muteins which could be seen in cyclic voltammetry experiments using the aforementioned diaphorase activity assay. The heterogeneous electron-transfer rate constant was determined for the copper

Table 2
Structures of self-assembled monolayers for the complexation of metal cations and subsequently histidine-tagged biomolecules.

Self-assembling molecule	Γ_{SAM} [pmol cm^{-2}]	Metal cation	Γ_{Me} [pmol cm^{-2}]	His-tagged biomolecule	$\Gamma_{His\text{-}tagged\ biomolecule}$ [pmol cm^{-2}]	Reference
(a) NTA terminated SAMs						
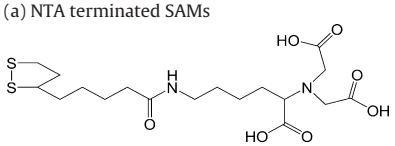	350 ± 25	Cu^{2+}	250 ± 50	Laccase (affinity binding constant of 2.2×10^7 M^{-1})	2.7 ± 0.1	[26]
	350 ± 25	Ni^{2+}	163	Human neuroglobin		[27]
	360 ± 30[a]	Cu^{2+}	280	Ferredoxin:NADP$^+$ reductase		[5]
	310 ± 25[a]	Co^{2+}		Ferredoxin:NADP$^+$ reductase		[28]
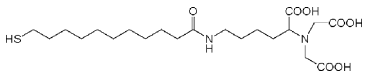	310 ± 25[a]	Co^{2+}		Horseradish peroxidase		[28]
		Ni^{2+}		Maltose binding protein		[30]
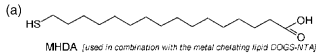						
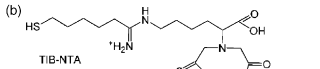		Ni^{2+}		Major urinary protein I		[29]
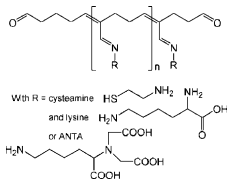		Ni^{2+}	~2000[a]	Single-chain Fv antibody fragment		[31]
		Ni^{2+}		Photosystem II	1.2[a]	[8]
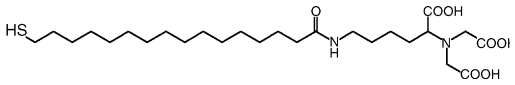		Ni^{2+}		Photosystem II	0.37	[34]
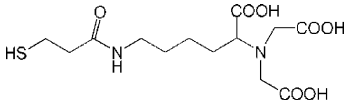		Ni^{2+}, Zn^{2+}	716[a]	Cytochrome c oxidase		[9,11,41,42]
		Ni^{2+}		Bacterial photosynthetic reaction center	4.8 ± 0.2	[10,35]
		Ni^{2+}		Photosystem I/hydrogenase complex	1.6 (hydrogenase)	[37]
		Ni^{2+}		Sensory rhodopsin II		[38]
		Ni^{2+}		Nanoscale apolipoprotein bound bilayer particles		[40]
(b) A macrocyclic triazacyclononane as NTA alternative						
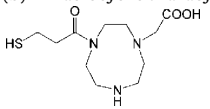		Zn^{2+}, Ni^{2+}		Thioredoxin, plastocyanin, cytochrome P450c17		[43,44]
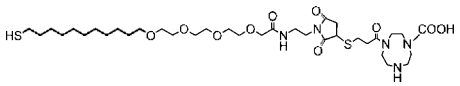		Ni^{2+}		Membrane scaffold protein		[45]

Γ = maximal surface coverage.
[a] Values have been converted to make units comparable.

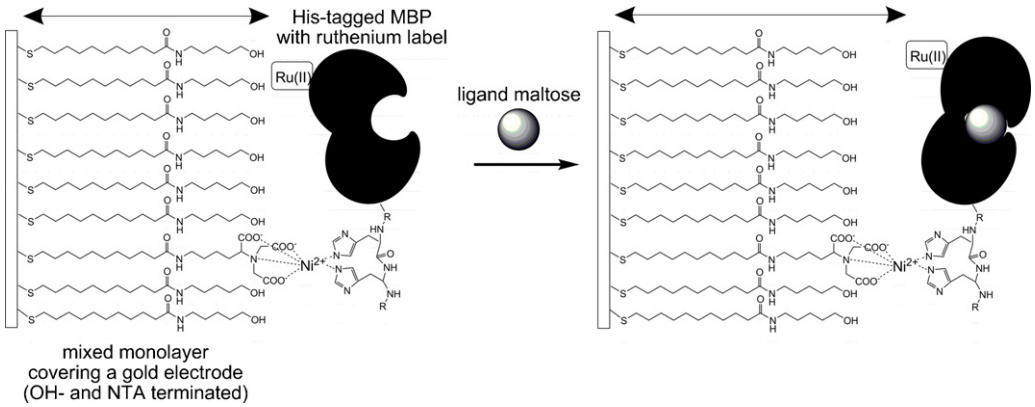

Fig. 2. Immobilization of His-tagged and Ru(II) labeled maltose binding protein (MBP) at a alkanethiol modified gold electrode [30]. MBP performs a hinge-bending motion upon ligand binding which increases the distance between the redox active Ru(II) and the electrode (indicated by an arrow).

loaded TOA-ANTA electrode immobilizing FNR (0.05 ± 0.01 cm s^{-1}) at a total protein surface coverage of $4.4 \pm 0.7 \times 10^{-12}$ mol cm^{-2}, a fixed ferricinium methanol concentration and varied NADPH concentrations ranging from 2.5×10^{-4} to 5×10^{-3} M. The authors prepared a monolayer containing covalently linked ferrocene besides ANTA (10:1) and immobilized the two FNR muteins I and II which differ in the position of the histidine pair. Only FNR-II showed catalytic activity in the presence of NADPH while FNR-I additionally needed the mediator ferricinium methanol. This indicates that FNR-II, which has the electron exchanging site of the isoalloxazine ring facing towards the electrode due to the position of the histidine pair, is directly wired to the gold electrode via the ferrocene units while FNR-I, with the electron exchanging site facing away from the electrode, is catalytically active but does not communicate with the gold electrode [5]. The immobilization of FNR via the TOA-ANTA system has also been transferred to gold nanoparticles as solid support [28]. Additionally the authors tested the immobilization of histidine-tagged horseradish peroxidase (HRP) with this system. Immobilization of the histidine-tagged HRP was proven by an activity assay employing 2,2′-azino-bis(3-ethylbenzothiazoline-6-sulfonic acid) (ABTS). The HRP is oxidized by hydrogen peroxide and subsequently reduced by ABTS. ABTS itself has a strong adsorption band at 405 nm in its oxidized state which is monitored here. The authors state that the enzymatic activity is retained when immobilizing the HRP enzyme at the nanoparticles while the supernatant does not show any enzymatic activity anymore signifying quantitative protein binding. When HRP without histidine-tag was used no absorbance increase was monitored indicating that binding only takes place via the histidine cobalt coordination. Furthermore FNR binding to the modified nanoparticles was proven via the diaphorase activity assay and unspecific protein binding did not occur.

In another study the mouse major urinary protein I (MUP-I), which belongs to a class of small carrier proteins called lipocalins and is a pheromone binding protein, was immobilized onto a Ni-NTA surface [29]. The SAM molecules used in this study were 16-mercaptohexadecanoic acid [MHDA] in combination with the metal chelating lipid 1,2-dioleoyl-*sn*-glycero-3-[(N-(5-amino-1-carboxypentyl)iminodiacetic acid)succinyl]nickel salt (DOGS-NTA-Ni^{2+}) and 1-thio-4-imino-butan-[N-(5-amino-1-carboxypentyl)iminodiacetic acid] (TIB-NTA) (Table 2). Two isoforms of histidine-tagged MUP-I were tested, one being the wild type (MUPwt) and one variant having the cd loop of the wild type replaced by the cd loop of the lipocalin retinol binding protein (MUPcd). When using the DOGS-NTA-Ni monolayer in a QCM experiment MUPwt showed typical binding properties since it attached strongly to the nickel cations and could be washed away by 200 mM imidazole. MUPcd instead bound irreversibly to the surface and elution with imidazole was not possible. The authors switched to the second monolayer system, TIB-NTA. Here less nickel was bound to the surface indicating a reduced packing of the monolayer. Furthermore binding of MUPwt on the TIB-NTA surface could not be reversed by imidazole treatment anymore. The authors assume an integration of the protein into the less densely packed TIB-NTA monolayer to a small extent which would result in a stronger protein binding than to DOGS-NTA-Ni^{2+}.

Benson et al. [30] prepared gold electrodes with a monolayer of 11-thioundecanoic acid which was further modified with carbodiimide to couple to lysine–triacetate and 5-aminopentanol (Table 2). The resulting surface presents NTA and hydroxyl groups and has been charged with nickel to create an immobilization scaffold for bacterial periplasmic binding proteins (bPBPs) (Fig. 2). The authors want to create an immobilization method generally applicable to proteins exhibiting allosteric interactions, which is a common feature of all bPBPs. Here the maltose-binding protein (MBP) was used that converts between its open ligand-free form to the closed ligand-bound form via a hinge-bending motion. The MBP exposes a C-terminal His-tag and binds to the nickel loaded electrode close to the hinge region. At the MBP side facing the electrode a ruthenium redox reporter group was introduced. The ligand binding site of MBP faces the bulk solution and upon ligand binding the system converts to the closed form which results in an increased distance between the ruthenium reporter group and the electrode surface. This event is measurable electrochemically since the electronic coupling between the electrode and the reporter group is altered. The binding of the electroactive MBP was proven by cyclic voltammetry. At fast scan rates of 4 V s^{-1} redox peaks for Ru(II) were observed with only small peak separation while unlabeled MBP did not give a signal. Furthermore the obtained midpoint potential of +220 mV vs. Ag/AgCl is similar to that of ruthenium bound directly to the monolayer and differs from the midpoint potential measured for Ru(II) labeled MBP in solution. The authors state multilayer protein formation is unlikely since electrochemical data indicate a MBP surface coverage of 10–30%. Without the His-tagged protein, nickel or the terminal NTA-groups or upon imidazole treatment no signals in cyclic voltammetry experiments could be seen. Ligand binding was monitored by alternating current voltammetry. Upon maltose binding the initial current of 12 μA decreased to 4 μA since the Ru(II) reporter group moved away from the electrode surface. The electrochemical response was ligand specific since addition of glucose, glutamine or zinc did not alter the signal. Furthermore the signal exposed a strong ligand concentration dependency. This immobilization approach was also tested with glucose- and glutamine-binding protein and similar electrochemical behavior and responsiveness towards ligand binding could be observed. Muteins of MBP with less affinity to maltose and a mutein

exposing zinc binding affinity instead of maltose have been tested successfully. Also the sensors showed good performance in real samples like beer and rat serum. The authors emphasize that in contrast to standard protein-based electrochemical sensors this system is not based on detecting enzymatic activity. The transduction mechanism remains the same for detecting different analytes and binding specificity can be engineered, as was shown for the MBP mutein binding zinc.

Maly et al. deposited thin transparent gold layers on glass and plastic supports by a sputtering technique [31]. Afterwards a self-assembled monolayer of cysteamine was formed on the gold surfaces exposing amine groups to the solution. These surfaces were used to create a chelator surface by adding sequentially glutaraldehyde, lysine, glutaraldehyde, ANTA and nickel sulfate (Table 2). It should be mentioned that in another study the procedure for surface modification could be improved by depositing the cysteamine layer electrochemically [32]. The amount of nickel bound to the surface has been improved 15–30-fold. But the authors point out that the structure of the electrochemically deposited cysteamine layers will be different from the chemically prepared ones since the electrochemical treatment is fast and does not allow preliminary self-assembly of the cysteamine. It results in the formation of disordered, compact and rigid multilayers. Interestingly Maly et al. used the glutaraldehyde modification protocol also for graphite electrodes. To introduce amine groups the graphite electrodes were treated with 3-aminopropyltriethoxysilane which makes gold sputtering unnecessary. The amount of nickel bound to the chemically prepared SAM was determined by adsorptive cathodic stripping voltammetry and revealed high surface densities (122 ± 3.0 ng cm^{-2}). The authors immobilized the single-chain Fv antibody fragment (scFv) which has been modified with an alkaline phosphatase (AP) activity before the His_6-tag at the C-terminal end (scFv-AP-His). After 16 h of sample incubation time a preconcentration of the histidine-tagged protein on the sensor surface out of the bacterial lysate was possible. Thereby the chelator surface with the lysine spacer showed less unspecific binding than one prepared without the spacer. Experiments aiming to reduce the unspecific binding by blocking with milk or BSA did also reduce the specific binding capacity. The activity of the immobilized scFv could be proven electrochemically by using ascorbate-2-phosphate as substrate. Additionally the histidine-tagged photosystem II (PSII) isolated from *Synechococcus elongatus* has been immobilized on a nickel NTA SAM which was prepared according to the procedure described before [8]. PSII can split water to produce electrons, oxygen and protons and possesses a high conversion efficiency [33]. The reaction of PSII is initiated by light which makes it an ideal test system since electrochemical interferences can be excluded when comparing signals of experiments with and without light exposure. PSII activity was measured amperometrically by using the artificial electron acceptor duroquinone, which is reduced by PSII upon light exposure and reoxidized at the screen printed gold working electrode. The PSII was immobilized in combination with BSA and yielded a maximum current of 1 nA whereas a pure PSII immobilization without BSA leads to current maxima of around 100 pA [8]. When treating the electrodes with imidazole in both cases the current signal decreased due to the histidine-tagged PSII being removed by the histidine-competitor imidazole. Interestingly in case of the PSII immobilization without BSA first an increase in current was observed. The authors relate this phenomenon to the structure of the densely packed PSII system being disturbed by the imidazole treatment. By decreasing the surface density of PSII for a short period of time, improved diffusion for duroquinone establishes. Since the amount of PSII further diminishes the current behaves analogous after the point where mass transport of the reduced duroquinone to the electrode is at its maximum [8]. It should be mentioned that the authors assume that an artificial bilayer might be present since PSII is naturally embedded in the thylakoid membrane and the PSII molecules may carry certain amounts of lipid molecules.

The histidine-tagged PSII of *Thermosynechococcus elongatus* was immobilized at gold surfaces modified with 1-octanethiol and 16-mercaptohexadecanoic acid (100:1) by Badura et al. [34], the latter being activated with carbodiimide to couple to ANTA (Table 2). PSII binding to the nickel NTA surface has been monitored by surface-enhanced infrared absorption spectroscopy (SEIRAS) and seems to come to saturation at around 15 min. Surface coverage of PSII has been estimated by SPR measurement in a flow cell. A maximal surface coverage of around 0.37 pmol PSII cm^{-2} was determined resulting in a specific coverage of 78% with an unspecific binding of 2%. These values correspond to a PSII monolayer coverage. The alkanethiol employed in this system is rather long and direct electron transfer is not efficient. Therefore the authors used the mediator 2,6-dichloro-1,4-benzoquinone (DCBQ) in electrochemical experiments. In cyclic voltammetry a redox wave for DCBQ was obtained which increased in its anodic current in presence of the immobilized PSII when exposed to light. Under these conditions DCBQ is reduced by PSII and the resulting increase of the anodic current can be seen which is related to the oxidation of the mediator. Without PSII or without light no increase in current has been monitored. An oxygen evolution rate of 6430 O_2 Chl^{-1} h^{-1}, a turnover rate of 4 ms per reaction center and an average current density of 14 μA cm^{-2} have been determined. This value is approximately 1200 times higher than the current density obtained by Maly et al. When the authors compare their results with the work of Maly et al. [8] they see several reasons for the superior performance of their immobilization assembly. Most important in this study a monolayer is formed while for the work of Maly et al. the deposition of a protein multilayer can be expected. Multilayer formation will go along with increased unspecific binding of PSII and mediator diffusion to the electrode will be hindered. Furthermore Badura et al. [34] assume that the choice of a different mediator may have had a beneficial influence.

Furthermore a monolayer consisting of dithiobis(N-succinimidyl propionate) (DTSP) coupled to ANTA has been used to immobilize His-tagged PSII on gold nanoparticles [33]. The monolayer–chelator combination DTSP–ANTA used in this study (Fig. 2) is a prominent example and a lot of immobilization approaches make use of this system. To conclude for PSII, it is interesting to mention that the degree of photocurrent enhancement measured corresponds to the increase in the active area of the electrode surface, which indicates that the rather big protein complex PSII can interpenetrate the nanospace of the gold nanostructures [33].

4.2. The DTSP–ANTA system

The commercially available dithiobis(N-succinimidyl propionate) (DTSP) molecule is commonly assembled on gold electrodes when an additional modification of the underlying monolayer is needed. DTSP itself contains an activated carboxylic acid group as tailgroup making an additional activation step unnecessary. This molecule is often used in combination with the chelator ANTA forming an amide bond between both and yielding a NTA terminated SAM (Fig. 3).

4.2.1. Immobilization of photosynthetic reaction center

The DTSP–ANTA monolayer system was also established for the immobilization of the photosynthetic reaction center (RC) from *Rhodobacter sphaeroides* having a His_7-tag at the C-terminal end of its M-subunit [10]. The orientation was chosen to present the primary donor, which is a dimer of bacteriochlorophylls, in direction of the electrode mimicking RCs native complex with cytochrome

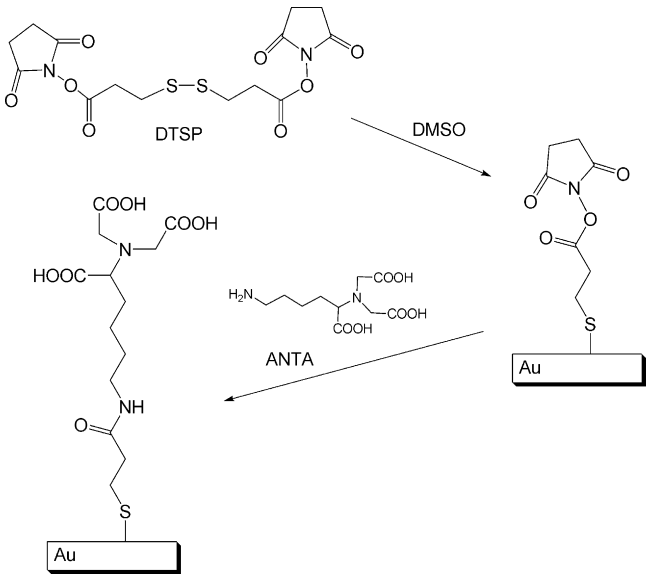

Fig. 3. Self-assembly of DTSP on a gold electrode followed by the coupling of ANTA yielding a NTA terminated SAM [7].

[10]. The authors used ubiquinone-10 as electron acceptor which can effectively accept electrons from the RC. The Ni–NTA terminated SAM has a length of approximately 17 Å which is long enough to enable spatial flexibility of the protein. In cyclic voltammetry experiments an irreversible oxidation peak at +700 mV vs. NHE was detected which was related to the oxidation of the primary donor. The authors give the information that in solution the midpoint potential for the primary donor is around 480 mV and describe that in another study also an irreversible oxidation peak at +900 mV was obtained when the RC has been immobilized in a thin lipid film on a graphite electrode. The authors cite that this shift in potential upon immobilization is probably due to a combination of kinetic effects of chemical and electrode reactions, electrode double layer effects and lipid–RC interactions [10]. Integration of the oxidation peak obtained in the cyclic voltammogram yields a surface coverage of immobilized RC of $4.8 \pm 0.2 \times 10^{-12}$ mol cm^{-2} which corresponds to an estimation of the surface coverage based on the protein size of 5×10^{-12} mol cm^{-2}. Ellipsometric measurements revealed a thickness of 37 ± 4 Å for the RC immobilized on the Ni–NTA SAM coated gold substrate which is less than the expected 60 Å which should be obtained for full surface coverage. The authors assume an incomplete surface coverage and consider a flatting of the protein upon immobilization as rather unlikely since the immobilized protein is photochemically active. Elution with 200 mM imidazole yielded a reduced photocurrent with an 80% decay compared to the initial value. Electron transfer in this system could be improved by addition of a second electron transfer protein, cytochrome c [35]. With the single point attachment via its His-tag the RC protein may tilt, rotate or lie down on the SAM surface. Cytochrome c will bind to the RC establishing an adequate electron transfer (ET) complex at the primary donor site [35].

This approach was further investigated by using carboxyl-terminated alkanethiols of different chain lengths [36]. After self-assembling on gold the molecules have been further modified to yield a terminal NTA group by performing a coupling reaction with 1-ethyl-3-(3-dimethylaminopropyl)carbodiimide (EDC) and ANTA. The linkers tested consisted of 3, 6, 10 and 15 methylene units. SAM formation was monitored by ellipsometry. After protein immobilization a RC surface density of approximately 3×10^{-12} mol cm^{-2} was determined by fluorescence analysis of pigments extracted from the electrode surface. Cyclic voltammetry experiments performed in the dark revealed that the RC immobilized at the NTA-SAM is electroinactive between −300 and +400 mV vs. NHE when the electron acceptor Q2 and cytochrome c are absent. It is also indicated that the RC-SAM assembly does block the interaction between Q2 and the electrode. At more positive potentials additionally a redox peak for immobilized RC was detected with a reversible redox couple at +500 mV vs. NHE. This corresponds to the midpoint potential determined by redox titration for the RC primary donor in solution and indicates that redox properties of RC are not altered when the protein is immobilized. Integration of the redox peaks yielded a surface coverage of approximately 4×10^{-12} mol cm^{-2}. At slow scan rates, e.g. 20 mV s^{-1}, a large peak to peak separation of 190 mV was monitored indicating a slow electron transfer between the electrode and the primary donor. The authors relate this effect to the location of the primary donor which is positioned approximately 11 Å away from the protein surface inside the protein. Building a complex with cytochrome c shifted the redox potential of the RC primary donor to 470 mV vs. NHE and decreases the peak to peak separation by 60 mV signifying an increased electron transfer rate due to a favorable protein orientation. The measured photocurrent upon illumination was strongly dependent on the SAM linker length. The current or rate constant decreased with the distance to the electrode while at short distances to at around 10 Å it was almost independent of the distance [36]. The authors analyzed the decay of electron transfer on the distance to the electrode and obtained a distance-dependency factor for the electron transfer from RC to gold of $\beta = 0.8$ per methylene unit of the SAM. The authors state that extrapolation to a distance of zero gives the maximal rate constant for electron tunneling between the flat gold electrode and the primary donor in the RC-cytochrome c complex about $k_0 = 10^4$ to 10^5 s^{-1} [36]. But there can be factors eliminating the rate of electron transfer for immobilized RC to the electrode at short distances which might be charge transfer within the protein or between the protein and the electrode. The authors also estimated the reorganization energy. Under reducing conditions at short distances the results showed low reorganization energy for on, off and steady state photocurrent of $\lambda = 0.21$–0.23 eV [36]. This value was similar to that estimated for electron transfer within the protein in solution by differential absorption spectroscopy and confirmed that the protein–short SAM–electrode complex has a rigid structure and does not show a strong conformational change upon electron transfer [36]. At longer distances from the electrode increases in the reorganization energy have been observed by the authors which they assume to be related to the flexibility of the linker or protein tilting [36].

Krassen et al. [37] immobilized a hybrid complex of photosystem I (PSI) and an oxygen-tolerant membrane-bound hydrogenase (MBH) from *Ralstonia eutropha* at a DTSP–ANTA modified gold electrode (Table 2). The special feature of the hybrid complex is the orientation of MBH to PSI via a subunit of PSI. The PSI used in this study lacks this subunit. Instead of that the subunit has been fused to the MBH, in close proximity to its electron transferring subunit, and both parts do spontaneously recombine yielding functional proteins. A decahistidine-tag has been engineered to the PSI part of the hybrid complex. Electron transfer occured from the gold electrode to PSI via the mediator N-methylphenazonium methyl sulfate (PMS) and upon illumination electrons are further transported to the hydrogenase unit which reduces protons to yield molecular hydrogen. Binding to the electrode surface was proven by SEIRAS and proved to be completed after 2 h. In SPR measurements the hydrogenase alone showed only weak unspecific binding to the Ni-NTA surface. 37% of the signal obtained is related to unspecific binding of MBH to PSI. A MBH coverage of 2.5×10^{-12} mol cm^{-2} was determined which implies a value of 1.6×10^{-12} mol cm^{-2} related to specific binding of MBH to PSI. In amperometric measurement the maximal photocurrent for the

assembly was recorded. The monolayer of PSI alone gave a maximal current density of 55 nA cm^{-2} while a bare gold electrode does not show any photocurrent. The authors assume the photocurrent may result from the formation of reactive oxygen species or more likely the direct reduction of PMS and protons at the acceptor site of PSI, which is exposed to the solution when MBH is not bound. Addition of MBH raises the photocurrent to 85 nA cm^{-2} indicating 30% of the measured photocurrent being related to H_2 production. Functional integrity of PSI was further confirmed for the PSI monolayer and the whole complex by performing action spectra, which means plotting the measured photocurrent against the applied wavelength. In both cases maximal photocurrent was observed at 685 nm indicating the photocurrent originating from PSI which is not influenced by MBH binding. Additionally the authors performed analytics with gas chromatography to detect the reaction product H_2. The immobilized hybrid complex exhibits a H_2 production rate of 120 ± 30 pmol s^{-1} cm^{-2} upon light exposure and when applying a constant potential of −90 mV, which is needed for PMS mediator reduction. After 30 min the measured photocurrent decreased to 50% of its initial value. Interestingly also the immobilized PSI without MBH showed a H_2 production rate of 31 ± 12 pmol s^{-1} cm^{-2}. The bare electrode and MBH alone did not show any significant H_2 production rates. Based on these data a specific surface activity of 4500 ± 1125 mol H_2 min^{-1} mol^{-1} has been determined which is in range with values obtained for MBH directly immobilized at graphite electrodes. In comparison with the latter approach the authors emphasize that with the immobilized hybrid PSI MBH complex it has been possible to drive the reaction at higher potentials and pH and less elevated temperatures [37].

4.2.2. Immobilization of rhodopsins

The histidine-tagged membrane protein sensory rhodopsin II (SR II) from *Natronomonas pharaonis* has been immobilized at gold electrodes modified with the DTSP–ANTA system (Table 2) by Jiang et al. [38]. SR II monolayer formation on the Ni–NTA surface was accompanied by direct reconstitution of the membrane protein into a lipid bilayer. The authors used surface-enhanced IR difference absorption spectroscopy (SEIDAS) to elucidate structural changes of the protein and its cofactor retinal with the additional possibility to detect single ion transfer events. Vibrational changes in the SEIDAS difference spectra were obtained for the immobilized SR II revealing differences between the light exposed and the dark state. Of main interest are bands related to the cofactor retinal, the protein backbone (amide I bands of peptide bonds) and amino acid side chains (carboxylic acid and amide residues). Upon light exposure SR II shows a proton pumping function [39]. Thereby the retinal Schiff base is donating a proton to the carboxylic acid side chain of an aspartic acid amino acid (D75). The band corresponding to the C=O stretching vibration of the carboxylic acid residue of D75 is of special interest since it gives evidence of the protonation state of the carboxylic acid group. With the protein monolayer modified gold electrode operated as working electrode the authors tested the influence of changes in the electric field across the SR II monolayer on the proton transfer reaction [38]. While at potentials higher than +200 mV vs. NHE the SEIDAS spectra does not change with the applied potential, for lower potentials a gradual decrease in intensity of the C=O stretching vibration band has been seen. At a potential of −300 mV vs. NHE proton transfer is completely inhibited. The authors conclude that a barrier of −300 mV cannot be overcome by the energy introduced to the retinal cofactor through light exposure. Interestingly the authors also investigated SR II from *Halobacterium salinarum* and light induced SEIDAS spectra revealed structural changes between both proteins with inhibition of proton transfer taking place at less negative potentials than for SR II from *Natronomonas pharaonis*. The authors emphasize the general applicability of the SEIDAS method to investigate the function of membrane proteins displaying a membrane potential dependency.

Zaitseva et al. [40] used a different approach to immobilize rhodopsin at a DTSP–ANTA modified gold electrode (Table 2). While Jiang et al. bound a histidine-tagged rhodopsin to the electrode surface here the authors established histidine-tagged nanoscale apolipoprotein bound bilayer (NABB) particles which serve as scaffold for rhodopsin immobilization. Besides immobilization and orientation aspects the NABB particles also protect the protein from the metal surface and mimic its native lipid environment. NABB particles with rhodopsin were prepared before immobilization by incubating histidine-tagged apolipoproteins with rhodopsin and a phospholipid. For the NABB particles in solution data obtained from UV–visible absorption spectra and ATR-FTIR spectra suggest that 30% of the particles remain empty upon incubation with rhodopsin. The authors found that the rhodopsin NABB particles exhibit a pH dependent steady-state equilibrium between two different states of the photocycle, namely the signaling state Meta II and the inactive Meta I precursor state, which corresponds to results found for rhodopsins in native membranes. Furthermore the addition of a peptide, which represents a part of the G-protein transducin and has a high affinity to rhodopsin, shifts the equilibrium to the active Meta II state indicating the functional integrity of the rhodopsin receptor molecule incorporated in the NABB particles. Binding of the rhodopsin loaded NABBs to the Ni–NTA surface was achieved in a time course of 90 min. In this study also the SEIDAS methodology was employed. Difference spectra of the immobilized rhodopsin NABB assembly between the lit and the dark state showed typical bands for functionally intact rhodopsin. By comparing data from SEIDAS spectra obtained for the NABB assembly and ATR-FTIR measurements for pure lipid bilayers the authors assume a mainly parallel orientation of the NABB particles with respect to the gold surface having an average angle of $24 \pm 10^{\circ}$. Concluding Zaitseva et al. point out that the surface density of membrane proteins immobilized via NABBs will be less than for other approaches making use of lipid bilayers due to the bigger size of the assembly [40]. Nevertheless advantages of NABBs are evident and include the solubility of the particles in buffer systems, their stability over time, the lipid like environment they offer and the opportunity to specifically bind a membrane protein without the need for previous genetic engineering.

4.2.3. Immobilization of cytochrome c oxidase

The membrane protein cytochrome c oxidase (CcO) with a histidine-tag at the C-terminus of subunit I or II was immobilized at the aforementioned DTSP–ANTA system via nickel ion chelation on a silver or gold electrode (Table 2). An artificial lipid bilayer was reconstituted by incubating the bound protein with dodecyl maltoside and 1,2-diphytanoyl-*sn*-glycero-3-phosphocholine in buffer [41]. The small hydrophilic layer between the electrode and the reconstituted lipid membrane is sensitive to changes in proton concentration as a result of CcO enzyme activity [42]. With this approach proton and electron transfer reactions can be examined separately. The authors compared resonance Raman spectra and SERR spectra of cytochrome c oxidase in solution and in the bound state and concluded that the structures of heme α and α_3 and their interaction with the protein environment are not changed upon immobilization, in both the ferrous and ferric state [41]. Reversibility of the immobilization was shown by SPR and QCM studies [9]. The addition of CcO, with the His-tag at subunit II, to the copper loaded DTSP–ANTA coated electrode resulted in a thickness increase of 2.1 nm due to protein binding. Treatment with imidazole established the initial value of reflectivity obtained for the DTSP–ANTA system before protein binding proving the reversibility of the immobilization process [9]. Furthermore metal ion concentration bound to the DTSP–ANTA system was determined by QCM

measurements yielding a surface coverage of 42 ng cm^{-2} for copper binding. Each bound copper ion occupied an area of 16.5 $Å^2$ which correlates to the cross-sectional area of a DTSP–ANTA molecule of approximately 17 $Å^2$ meaning each NTA group is complexing one copper ion [9]. Furthermore the CcO immobilization on nickel loaded DTSP–ANTA coated gold electrodes and subsequent reconstitution into a lipid bilayer has been investigated in situ by SEIRAS [6,7]. When treating the electrode with imidazole almost all CcO was eluted and desorption kinetics was much faster than the adsorption process. Subsequently imidazole was removed by washing and His-tagged CcO could be immobilized again at the nickel chelating DTSP–ANTA surface but resulting in a reduced surface coverage of 60% compared to the initial adsorption value [7]. The different orientation of the His-tag and its influence on the electron transfer from the electrode was additionally investigated by time-dependent SERR by Hrabakova et al. [11]. The authors used zinc instead of nickel because it is electrochemically inert even at lower potentials. The authors point out that due to the relatively large separation between the redox sites and the electrode, for example by the solution phase between the monolayer and the bound protein, the true potential at the redox site will be different from the one applied at the electrode. A rate constant of $0.002 \pm 0.0005\ s^{-1}$ was determined for the reduction of immobilized CcO under anaerobic conditions up to a potential of −450 mV vs. NHE with the orientation of CcO having no influence on the rate constant. In contrast to Hrabakova et al., Friedrich et al. [42] state that direct electron transfer to the immobilized CcO is specifically controlled by the orientation of the protein. Only when the cytochrome c binding site of CcO is directed towards the electrode electrons are transferred via the primary electron acceptor Cu_A. In CVs a single reduction peak at −274 mV and a corresponding oxidation peak at −209 mV vs. NHE were obtained under anaerobic conditions. With increasing scan rate peak positions remained constant and the current densities increased linearly with the scan rate which is consistent with surface confined and fast electron transfer. Electron transfer seems to be facilitated by the Ni^{1+}/Ni^{2+} complex [42].

4.3. Alternatives to NTA

An alternative to NTA as chelating ligand is a macrocyclic triazacyclononane (tacn) (Table 2), more precisely 1-acetato-4-benzyl-triazacyclononane (Acbztacn) [43,44]. Similar to NTA the metal is ligated by four atoms of the chelating agent leaving two metal sites free for histidine coordination. Furthermore the Acbztacn chelating agent stabilizes the metal ligand interaction by a macrocyclic effect which additionally hinders metal leaching [44]. Johnson et al. prepared a gold electrode with the self-assembled monolayer mercaptopropionic acid and coupled the Acbztacn chelating agent via a carbodiimide reaction to the monolayer molecule. Nickel binding to the Acbztacn modified surface and a NTA surface have been compared by SPR measurements. Upon treatment with EDTA or at low pH the metal ions could be stripped from the NTA surface while for the Acbztacn surface no removal of metal ions could be seen. After 24 h in standard buffer for the NTA modified surface 20% loss of nickel cations was monitored. The Acbztacn surface revealed no changes under the same experimental conditions. The three histidine-tagged proteins thioredoxin, plastocyanin and cytochrome P450c17 have been immobilized on the Acbztacn surface showing only little unspecific protein binding (<5%) in the absence of nickel while for the NTA surface 20–50% of the total binding magnitude counted for unspecifically bound protein. Dissociation constants could only be determined for the NTA surface. The Acbztacn surface did not show any dissociation of the bound protein. The authors conclude that the Acbztacn surface shows a higher selectivity and specificity and a stronger chelator–metal–histidine interaction than the NTA surface. For all three histidine-tagged proteins an electrochemical communication could be seen between the electrode and the protein redox site in cyclic voltammograms and midpoint potentials of −300 mV (P450c17), −100 mV (thioredoxin) and +600 mV vs. NHE (plastocyanin) have been determined [44]. Furthermore for protein immobilized at Acbztacn the peak widths remained narrow indicating a uniform protein layer. With using zinc instead of nickel the protein Acbztacn assembly was electrochemically accessible over a wide potential range and for a longer time at different scan rates [44].

A similar approach was used to immobilize a hexahistidine-tagged membrane scaffold protein (MSP) at a thiol-terminated and nickel loaded triazacyclononane (Actacn) derived ligand [45] (Table 2). By addition of a lipid the membrane scaffold protein was used to create nanodiscs for reconstitution of the seven-transmembrane photoreceptor rhodopsin within the nanodisc assembly (Fig. 4). The basic idea of creating a histidine-tagged scaffold for protein immobilization can also be found in the work of Zaitseva et al. [40]. The thiol-terminated ligand was coupled to a monolayer exhibiting maleimide and tri(ethylene glycol) groups. While maleimide reacts readily with the thiol groups of the ligand creating a covalent bond between both the tri(ethylene glycol) groups are supposed to suppress unspecific interactions between proteins and the surface. By SPR measurements the binding of the nanodiscs to the nickel Actacn complex was proven and remained stable while washing with buffer. A special MALDI-TOF technique was applied (self-assembled monolayers for matrix-assisted laser desorption ionization time-of-flight mass spectrometry/SAMDI) revealing spectra with clear peaks for the membrane scaffold protein at $[M]^+$ at m/z 25.6 kDa and for the lipid molecule at 760.1 Da [45]. Immobilization of nanodiscs containing rhodopsin showed the same peaks for the membrane scaffold protein and the lipids and showed an additional peak at $[M]^+$ at m/z 43.6 kDa for rhodopsin. Additionally the authors performed a functional assay based on rhodopsin binding the transducin protein complex upon light exposure. A SAMDI spectrum of the according sample showed an additional peak for transducin while a control experiment conducted in the dark did not yield any additional peak besides MSP and rhodopsin.

5. Further electrode surface modification methods

Wang et al. used functionalized single-walled carbon nanotubes (SWCNTs) to immobilize His-tagged NADH oxidase of *Bacillus cereus* [46]. The surface of the SWCNTs was activated by an acid treatment introducing carboxylic acid functionalities which were modified subsequently with ANTA via a carbodiimide mediated reaction. NADH oxidase could be immobilized specifically via cobalt cations out of the crude cell lysate and remained stably bound to the surface for 1 week. Loading capacity of the SWCNTs was determined to be around 0.47 mg enzyme per mg SWCNTs [46]. The authors found that the immobilized NADH oxidase retained 92% of its native maximum activity and the K_M value determined is the same than for the enzyme in solution. Interestingly the storage stability of the immobilized NADH oxidase exceeds the stability of the free enzyme and still shows 70% of its initial activity after 40 days of storage at 4 °C. Furthermore the immobilized enzyme was still active at elevated temperatures up to 90 °C whereas the enzyme in solution was already denatured at 70 °C. The enzyme could be eluted by imidazole treatment and loading capacity and activity remained almost the same after binding of fresh enzyme. This work has been extended to multi-walled carbon nanotubes (MWCNTs) and carbon nanospheres (CNSs) and enzyme immobilization showed to be specific and enzyme activity could be retained [47].

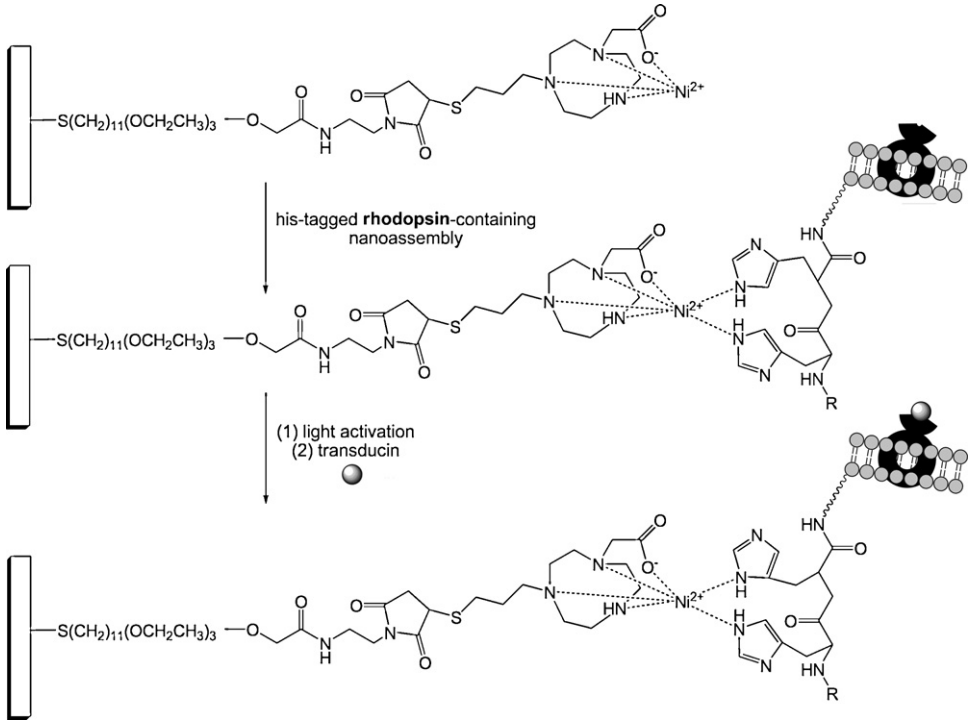

Fig. 4. Immobilization of a nanodisc, among others consisting of a histidine-tagged membrane-scaffold protein, containing rhodopsin and subsequent binding of transducin upon light exposure [45].

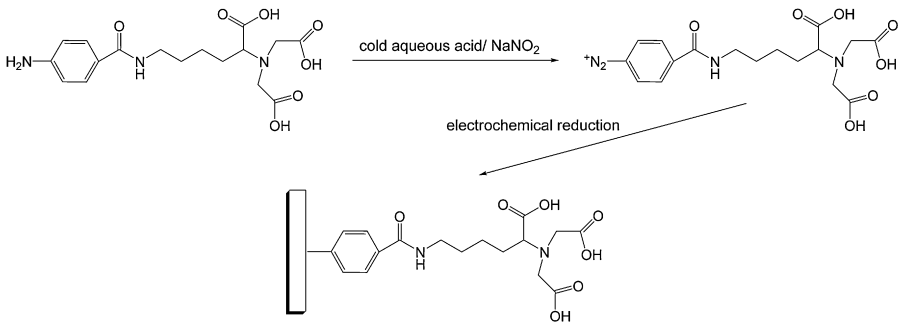

Fig. 5. Grafting of a carbon electrode by electrochemical reduction of a diazonium salt [4].

Another possibility to modify carbon surfaces is the grafting with diazonium salts which are derived from aminophenyl derivatives of iminodiacetic and nitrilotriacetic acid [4]. The grafting is done electrochemically and has the advantage of creating chelating electrode surfaces fast and in a one step reaction with a low background current and a defined amount of deposited ligand (Fig. 5). The authors bound copper to the chelating electrode and immobilized histidine-tagged horseradish peroxidase and histidine-tagged green fluorescent protein. In another study this approach was used to immobilize a histidine-tagged and non-glycosylated glucose oxidase variant and fast direct electron transfer with the electrode was shown [48].

Another rather different method was developed by Haruyama et al. [49]. The authors introduced a short peptide tag consisting of histidine residues, which they call ECtag, at several model proteins [49,50]. The protein bearing the ECtag was incubated with nickel or copper cations which subsequently were reduced at a platinum electrode resulting in immobilization of the protein. The immobilized protein remained stable at the surface of the electrode when no potential was applied but upon application of an anodic potential the protein could be completely removed due to nickel or, respectively, copper oxidation.

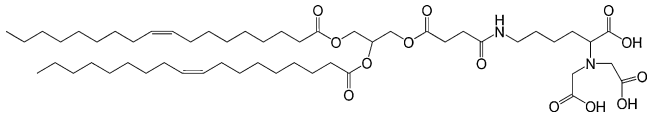

Fig. 6. The metal chelating lipid DOGS-NTA.

Johnson et al. [51] deposited cysteine and the short chain homopolymer poly(L-cysteine) at glassy carbon electrodes. Both surface modifications showed metal binding capacities and for poly(L-cysteine) bound metal ions could be removed upon application of repetitive oxidative pulses. The assembly has been compared with a glycine modified electrode which showed only minimal metal binding.

Furthermore metal chelating lipids have been used for immobilization of histidine-tagged proteins (Fig. 6), also in combination with self-assembled monolayers on gold electrodes [29]. On silica surfaces DOGS-NTA has been established with 1,2-dioleoyl-*sn*-glycero-3-phosphocholine (DOPC) [52]. In the latter case the lipid bilayers were prepared by spontaneous fusion of vesicles on

the hydrophilic silica surface. After chelation of nickel cations a histidine-tagged antibody fragment was immobilized and the immobilization process was detected acoustically.

6. Outlook

Besides the aforementioned methods there are still additional approaches that established a surface modification for metal ion chelation but which have not yet been tested with histidine-tagged biomolecules or the whole set up has not yet been transferred to an electrode substrate. This includes the experimentally facile method of entrapping a chelating agent into a growing conductive polymer network, which has been done for ethylenediamine tetra-acetic acid (EDTA) in polyaniline [53] or 3-(2-pyridyl)-5,6-diphenyl-4,4′-disulfonate-1,2,4-triazine ($PDTDS^{2-}$) [54] and 2,6-pyridine dicarboxylic acid (PDCA) [55] in polypyrrole. This approach may be limited by a partial expulsion of the entrapped negatively charged counter anions as well as the low conductivities of the resulting polymer films. The latter can be prevented when entrapping the chelating agent only in the outer part of the polymer, as shown for NTA in polyaniline [56]. Furthermore the chelating group can be grafted to the outside of the polymer, for example by entrapping poly(acrylic acid) and modifying it with a histidine containing oligopeptide [57]. Besides polymers with carboxylic acid groups also pyrrole monomers with β-diketones as complexing groups have been tested for metal ion immobilization [58]. Furthermore, a terthiophene polymer was used for metal cation detection after covalently grafting of EDTA via a carbodiimide reaction [12,59]. Additionally, grafting with an imidazole derivative is possible as shown with a pentafluorophenol ester derivative of 3-(pyrrole-1-yl)propanoic acid (PPA) [20] resulting in a modified polypyrrole capable of nickel binding. The same monomer can be grafted with cysteamine instead of an imidazole derivative which creates a polymer bearing a free thiol group [21]. A free thiol group is a strong ligand for metal cations and could also be shown to bind soft metal cations such as platinum. Additionally the metal cation remained stably bound to the cysteamine modified polypyrrole at low pH and in presence of competing amine ligands [21].

Besides approaches to detect metal cations many studies aim to elucidate the immobilization process itself and are not related to electrochemistry. But since common analytical techniques like ellipsometry and surface plasmon resonance measurements require a gold substrate it suggests to transmit these surface modification approaches to an electrode. For example the NTA-terminated alkanethiol N-[5[(3,6,9-trioxaeicos-19-en-1-yl)oxy]carbonyl]iminodiacetic acid was used in combination with an tri(ethylene glycol) terminated SAM to immobilize nickel cations and subsequently a histidine-tagged three-domain single-chain T-cell receptor construct, the human TATA box binding protein, the transcriptional activator Gal 4 and two components of the yeast RNA polymerase II holoenzyme–TFIIB and Gal 11 [3]. All proteins bound well and interacted with solution species. The influence of the multivalency of the chelator was tested by Valiokas et al. who used several alkanethiols with mono-, bis- and tris-NTA moieties [60]. Tris-NTA performed best for a hexahistidine-tagged extracellular receptor subunit as model protein. The anti-lysozyme F_{ab} fragment with a hexahistidine-tag at the C-terminus of its heavy chain was immobilized via nickel cations at a NTA-terminated SAM co-assembled with a hydroxythioalkane to control the surface density of the chelators as well as the negative surface charge [61]. Unspecific protein adsorption can be prevented when using tri(ethylene glycol) terminated alkanethiols in combination with the chelator molecules, as it has been shown for the immobilization of his-tagged epidermal growth factor [62].

Another interesting approach tested with SPR uses a β-cyclodextrine (β-CD) variant with seven heptathioether chains for self-assembling on gold [63]. β-CD is well known as host for several small organic molecules in aqueous solution and forms a dense and well ordered monolayer on gold. An adamantyl functionalized NTA ligand complexed to a metal cation was assembled at the β-CD surface. Afterwards three proteins differing in size and number of histidine-tag were studied: the maltose binding protein (MBP) with one hexahistidine-tag; the tetrameric, autofluorescent timer mutant of DsRed with one hexahistidine-tag at each monomer; 20S proteasome with 14 hexahistidine-tags inserted into the α subunits [63].

Concluding it has to be noted that up to now most work dealing with the immobilization of His-tagged biomolecules is focusing on sensor approaches. But also catalytic applications are conceivable in the future. Immobilizing a biocatalyst of interest at a solid electrode surface in a reversible fashion and driving a reaction electrochemically would be of great interest. For example downstream processing of the resulting product would be facilitated and cost for the natural cofactor of the biocatalyst could be spared.

7. Conclusion

The immobilization of histidine-tagged proteins on electrodes has been achieved by using a variety of different matrices. The most common one being self-assembled monolayers, which are easily prepared and offer interesting electrochemical properties, e.g. a low background current. Nevertheless also conductive polymers offer some advantages which include their switchable conductivity as well as the deposition which can be controlled electrochemically. Biomolecule immobilization on these surfaces via the histidine-tag metal–chelate interaction seems to be a promising approach. The immobilization is reversible allowing the regeneration of the surface. The flexible arrangement does not affect the biomolecule conformation. Some aspects of key impact, such as the stability of the His-tag assembly, are still far from being completely elucidated and are thus worth being further investigated in the future.

Acknowledgement

This study is financially supported by the EU-FP7 OXYGREEN research grant.

References

[1] R. Vallina-García, M. del Mar García-Suárez, M.T. Fernández-Abedul, F.J. Méndez, A. Costa-García, Biosens. Bioelectron. 23 (2007) 210.
[2] L.L. Martin, D.L. Johnson, Sensor Chips, US 2006/0194343 A1, 2006.
[3] G.B. Sigal, C. Bamdad, A. Barberis, J. Strominger, G.M. Whitesides, Anal. Chem. 68 (1996) 490.
[4] R. Blankespoor, B. Limoges, B. Schöllhorn, J.-L. Syssa-Magalé, D. Yazidi, Langmuir 21 (2005) 3362.
[5] J. Madoz-Gúrpide, J.M. Abad, J. Fernández-Recio, M. Vélez, L. Vázquez, C. Gómez-Moreno, V.M. Fernández, J. Am. Chem. Soc. 122 (2000) 9808.
[6] K. Ataka, B. Richter, J. Heberle, J. Phys. Chem. B 110 (2006) 9339.
[7] K. Ataka, F. Giess, W. Knoll, R. Naumann, S. Haber-Pohlmeier, B. Richter, J. Heberle, J. Am. Chem. Soc. 126 (2004) 16199.
[8] J. Maly, J. Krejci, M. Ilie, L. Jakubka, J. Masojídek, R. Pilloton, K. Sameh, P. Steffan, Z. Stryhal, M. Sugiura, Anal. Bioanal. Chem. 381 (2005) 1558.
[9] F. Giess, M.G. Friedrich, J. Heberle, R.L. Naumann, W. Knoll, Biophys. J. 87 (2004) 3213.
[10] S.A. Trammell, L. Wang, J.M. Zullo, R. Shashidhar, N. Lebedev, Biosens. Bioelectron. 19 (2004) 1649.
[11] J. Hrabakova, K. Ataka, J. Heberle, P. Hildebrandt, D.H. Murgida, Phys. Chem. Chem. Phys. 8 (2006).
[12] M.A. Rahman, M.-S. Won, Y.-B. Shim, Anal. Chem. 75 (2003) 1123.
[13] T. Ahuja, I.A. Mir, D. Kumar, Biomaterials 28 (2007) 791.
[14] S. Cosnier, Biosens. Bioelectron. 14 (1999) 443.
[15] N.K. Guimard, N. Gomez, C.E. Schmidt, Prog. Polym. Sci. 32 (2007) 876.
[16] N. Haddour, S. Cosnier, C. Gondran, J. Am. Chem. Soc. 127 (2005) 5752.
[17] C.L. Aravinda, S. Cosnier, W. Chen, N.V. Myung, A. Mulchandani, Biosens. Bioelectron. 24 (2009) 1451.

[18] J. Baur, C. Gondran, M. Holzinger, E. Defrancq, H. Perrot, S. Cosnier, Anal. Chem. 82 (2010) 1066.
[19] J. Baur, M. Holzinger, C. Gondran, S. Cosnier, Electrochem. Commun. 12 (2010) 1287.
[20] J. Davis, A. Glidle, A.E.G. Cass, J. Zhang, J.M. Cooper, J. Am. Chem. Soc. 121 (1999) 4302.
[21] A. Glidle, C.S. Hadyoon, A.E.G. Cass, J.M. Cooper, Electrochim. Acta 45 (2000) 3823.
[22] A. Glidle, M.J. Swann, N. Gadegaard, J.M. Cooper, Physica B 276–278 (2000) 359.
[23] F. Darain, C. Ban, Y.-B. Shim, Biosens. Bioelectron. 20 (2004) 857.
[24] Y. Li, W. Zhang, J. Chang, J. Chen, G. Li, Y. Ju, Macromol. Chem. Phys. 209 (2008) 322.
[25] A. Ulman, Chem. Rev. 96 (1996) 1533.
[26] V. Balland, C. Hureau, A.M. Cusano, Y. Liu, T. Tron, B. Limoges, Chem. Eur. J. 14 (2008) 7186.
[27] V. Balland, S. Lecomte, B. Limoges, Langmuir 25 (2009) 6532.
[28] J.M. Abad, S.F.L. Mertens, M. Pita, V.M. Fernández, D.J. Schiffrin, J. Am. Chem. Soc. 127 (2005) 5689.
[29] M.A. Rodgers, Sens. Actuators B 150 (2010) 12.
[30] D.E. Benson, D.W. Conrad, R.M. de Lorimier, S.A. Trammell, H.W. Hellinga, Science 293 (2001) 1641.
[31] J. Maly, E. Illiano, M. Sabato, M. De Francesco, V. Pinto, A. Masci, D. Masci, J. Masojidek, M. Sugiura, R. Franconi, R. Pilloton, Mater. Sci. Eng. C 22 (2002) 257.
[32] J. Maly, C. Di Meo, M. De Francesco, A. Masci, J. Masojidek, M. Sugiura, A. Volpe, R. Pilloton, Bioelectrochemistry 63 (2004) 271.
[33] N. Terasaki, M. Iwai, N. Yamamoto, T. Hiraga, S. Yamada, Y. Inoue, Thin Solid Films 516 (2008) 2553.
[34] A. Badura, B. Esper, K. Ataka, C. Grunwald, C. Wöll, J. Kuhlmann, J. Heberle, M. Rögner, Photochem. Photobiol. 82 (2006) 1385.
[35] N. Lebedev, S.A. Trammell, A. Spano, E. Lukashev, I. Griva, J. Schnur, J. Am. Chem. Soc. 128 (2006) 12044.
[36] S.A. Trammell, I. Griva, A. Spano, S. Tsoi, L.M. Tender, J. Schnur, N. Lebedev, J. Phys. Chem. C 111 (2007) 17122.
[37] H. Krassen, A. Schwarze, B. Friedrich, K. Ataka, O. Lenz, J. Heberle, ACS Nano 3 (2009) 4055.
[38] X. Jiang, E. Zaitseva, M. Schmidt, F. Siebert, M. Engelhard, R. Schlesinger, K. Ataka, R. Vogel, J. Heberle, PNAS 105 (2008) 12113.
[39] E. Pebay-Peyroula, A. Royant, E.M. Landau, J. Navarro, Biochim. Biophys. Acta 1565 (2002) 196.
[40] E. Zaitseva, M. Saavedra, S. Banerjee, T.P. Sakmar, R. Vogel, Biophys. J. 99 (2010) 2327.
[41] M.G. Friedrich, F. Gieß, R. Naumann, W. Knoll, K. Ataka, J. Heberle, J. Hrabakova, D.H. Murgida, P. Hildebrandt, Chem. Commun. (2004) 2376.
[42] M.G. Friedrich, J.W.F. Robertson, D. Walz, W. Knoll, R.L.C. Naumann, Biophys. J. 94 (2008) 3698.
[43] D.L. Johnson, S.W. Polyak, J.C. Wallace, L.L. Martin, Lett. Pept. Sci. 10 (2003) 495.
[44] D.L. Johnson, L.L. Martin, J. Am. Chem. Soc. 127 (2005) 2018.
[45] V.L. Marin, T.H. Bayburt, S.G. Sligar, M. Mrksich, Angew. Chem., Int. Ed. 46 (2007) 8796.
[46] L. Wang, L. Wei, Y. Chen, R. Jiang, J. Biotechnol. 150 (2010) 57.
[47] L. Wang, R. Xu, Y. Chen, R. Jiang, J. Mol. Catal. B: Enzym. 69 (2011) 120.
[48] S. Demin, E.A.H. Hall, Bioelectrochemistry 76 (2009) 19.
[49] T. Haruyama, T. Sakai, K. Matsuno, Biomaterials 26 (2005) 4944.
[50] H. Sakamoto, T. Haruyama, Colloids Surf. B 79 (2010) 83.
[51] A.M. Johnson, J.A. Holcombe, Anal. Chem. 77 (2005) 30.
[52] E. Gizeli, J. Glad, Anal. Chem. 76 (2004) 3995.
[53] J.H. Zagal, R.R. del Río, B.A. Retamal, S.R. Briaggio, J. Appl. Electrochem. 26 (1996) 95.
[54] D.W.M. Arrigan, M.J. Lowens, Electroanalysis 11 (1999) 647.
[55] G.G. Wallace, Y. Lin, J. Electroanal. Chem. 247 (1988) 145.
[56] J.A. Lori, A. Morrin, A.J. Killard, M.R. Smyth, Electroanalysis 18 (2006) 77.
[57] H. Zhang, S. Boussaad, N. Ly, N.J. Tao, Appl. Phys. Lett. 84 (2004) 133.
[58] S. Roux, P. Audebert, J. Pagetti, M. Roche, New J. Chem. 24 (2000) 877.
[59] M.A. Rahman, D.S. Park, M.-S. Won, S.-M. Park, Y.-B. Shim, Electroanalysis 16 (2004) 1366.
[60] R. Valiokas, G. Klenkar, A. Tinazli, A. Reichel, R. Tampé, J. Piehler, B. Liedberg, Langmuir 24 (2008) 4959.
[61] D. Kröger, M. Liley, W. Schiweck, A. Skerra, H. Vogel, Biosens. Bioelectron. 14 (1999) 155.
[62] T. Nakaji-Hirabayashi, K. Kato, Y. Arima, H. Iwata, Biomaterials 28 (2007) 3517.
[63] M.J.W. Ludden, A. Mulder, K. Schulze, V. Subramaniam, R. Tampé, J. Huskens, Chem. Eur. J. 14 (2008) 2044.